



# Application of Machine Learning Techniques for Predicting the Compressive Strength of GGBS-Based Geo-polymer Mortar

Ram Bahadur<sup>1\*</sup>, Arun Kumar<sup>2</sup>, Shreekanth Birgonda<sup>3</sup>, Ajay Kumar<sup>4</sup>

<sup>1\*</sup>Research Scholar, Civil Engineering, National Institute of Technology, Delhi, India

<sup>2</sup> Research Scholar, Civil Engineering, National Institute of Technology, Delhi, India

<sup>3</sup> Research Associate, Civil Engineering, National Institute of Technology, Delhi, India

<sup>4</sup>Associate Professor, Civil Engineering, National Institute of Technology, Delhi, India

Corresponding Author\*: Email Id: [rambahadur222@gmail.com](mailto:rambahadur222@gmail.com)

**Abstract:** The process of determining the ideal mixture of alkaline activators enables scientists to achieve higher compressive strength results for Geo-Polymer mortar with the use of Ground Granulated Ballast Furnace Slag (GGBS) that undergoes ambient temperature curing. The research used a combined methodology which included laboratory tests together with machine learning (ML) modeling to investigate how different sodium hydroxide (NaOH) concentrations from 6M to 14M sodium silicate(SS) ( $\text{Na}_2\text{SiO}_3$ ) Solution to The Sodium hydroxide (SH) (NaOH) solution ratio affected strength development. In this Study standard mortar production methods which required a consistent binder: sand (1:3) and an activator: binder (0.70). In experimental studies compressive strength at two distinct curing periods which were 7 and 28 days. In Experimental Result produced that compressive strength developed a distinct nonlinear pattern which depended on the sodium hydroxide solution concentration. The 7-day strength at lower molarities which ranged from 6M to 8M showed strength values between 22 MPa and 30 MPa. The 28-day compressive strength reached its highest points of 60 to 62 MPa when specimens received activation through 10 to 14 M NaOH solution, resulting in a 25 to 30 percent increase over the results from lower molarity solution mixes. In this study created predictive models by using experimental data which they obtained through Multiple Linear Regression (MLR) Model, a Support Vector Machine (SVM) Model, Random Forest Modeling (RF) and Extreme Gradient Boosting (XG-Boost) methods. The XG-Boost model achieved the best predictive performance which produced determination coefficients of approximately 0.97 at 7 days and 0.98 at 28 days together with minimal error measurements, which included RMSE below 1.7 MPa and MAE below 1.3 MPa. The research findings proved that machine learning methods based on ensemble techniques can precisely predict compressive strength, which enables reliable and sustainable methods to optimize concrete mixes and design GGBS-based geo-polymer mortars for performance.

**Keywords:** GGBS, Compressive Strength, Geo-polymer, Multiple Linear Regression, XG-Boost

## Abbreviations

$\hat{f}c_7, \hat{f}c_{28}$ : Compressive Prediction strength ( $\text{N/mm}^2$ ) 7 and 28 days.

$fc_7, fc_{28}$  : Compressive Experimental Strength ( $\text{N/mm}^2$ ) 7 and 28 days.

$M$ : NaOH molarity

$SS/SH$ : Sodium Silicate (SS) ( $\text{Na}_2\text{SiO}_3$ )/ Sodium Hydroxide ratio (SH) (NaOH)

$\beta_0, \beta_1, \beta_2$ : Regression coefficients

$N$ : Number of samples

$T$ : Number of trees

$K$ : Number of boosting iterations

$\alpha_i, \alpha_i^*$ : Support vector coefficient

$\gamma$ : Kernel parameter

$x_i$  : Training samples

$x$  : Input Vector

$h_t$  : Prediction of the  $t^{\text{th}}$  decision tree based on input parameters

$f_k$  : Prediction function of  $k^{\text{th}}$  tree

© The Author(s) 2026

A. Agnihotri et al. (eds.), *Proceedings of the Conference on Bridging Engineering Disciplines with AI and Machine Learning (BEDAIML 2026)*, Advances in Intelligent Systems Research 209,

[https://doi.org/10.2991/978-94-6239-697-5\\_13](https://doi.org/10.2991/978-94-6239-697-5_13)

OPC: Ordinary Portland cement

GGBS: Ground Granulated Blast Furnace Slag

## 1. Introduction

Construction industry experiences fast development, which creates a strong need for OPC. This material serves as a major source of carbon dioxide (CO<sub>2</sub>) emissions worldwide [1]. Production of OPC is very energy-consuming and emits almost 1 ton of CO<sub>2</sub> per ton of cement manufactured thus contributing to ecological pollution and contributing to weather change[2]. In response to these fears, the growth of low-carbon, more eco-friendly alternative binders has come into focus[3]. Of these options, geo-polymer material has become a potential group of cementitious binders with a lower carbon footprint, enhanced early high-strength, and improved mechanical and performance properties, owing to its superior mechanical and durability performance relative to traditional OPC systems[4]. The synthesis of geo-polymers occurs by means of alkaline activation of alumina-silicate-rich industrial by-products; this permits improving the valuation of the waste products, whilst reducing the environmental impact[5]. GGBS is widely used as a primary precursor material in geo-polymer systems because of its elevated calcium content, latent hydraulic reactivity, and finely divided particle structure, which collectively enhance early strength development and overall mechanical performance[6]. These properties facilitate fast geo-polymerization and early strength growth and GGBS-based geo-polymer mortar is specifically applicable to an ambient curing environment and realistic construction projects[7]. Chemical Structure of alkaline activated materials controls the mechanical properties of the systems. Concentration of Sodium Hydroxide (NaOH) and the ratio of Sodium silicate to Sodium Hydroxide ratio control the dissolution precursor material and chemical structure and Geo-polymeric gel phases impact the compressive strength of Geo-polymer mortar [8].

The dissolution process of GGBS alumina-silicate species depends on Sodium hydroxide (NaOH) molarity while calcium-alumina-silicate-hydrate (C-A-S-H) gel type binder production results from this process[9]. Low molarity can lead to inadequate dissolution and weak geo-polymeric networks and high molarity can lead to high reaction rates, instability of the microstructure and decreased performance over time[10]. Past studies show that the concentration of NaOH between 6M and 14M establishes a strong relationship with the development of compressive strength. However, researchers have not yet found the best combination of activators because the interactions between molarity and SS/SH ratio and strength development show nonlinear behaviour [11].

Conventionally, optimization of geo-polymer mix ratios is based on a time consuming and labour intensive and expensive trial and error method[12]. The traditional statistical methods face challenges when they attempt to measure the complex nonlinear relationships that dictate geo-polymerization reactions. The research from previous years demonstrates that machine learning (ML) and artificial intelligence (AI) methods can accurately predict cementitious materials' mechanical properties through their ability to directly learn from experimental data [13]. The multiple linear regression algorithm together with SVR, RF and XG-Boost models have proven superior performance to traditional regression models in their ability to model nonlinear behaviour and achieve precise prediction results [14].

The current research develops a machine learning solution which predicts Compressive strength of Geo-polymer mortar with the used of GGBS through NaOH molarity variations between 6M and 14M and SS/SH ratio changes. The first aim is to minimize the experimental work and increase the accuracy of prediction and allow the optimization of the geo-polymer mix design with the help of AI. The proposed method will help researchers create sustainable geo-polymer mortars which produce high performance with reduced carbon emissions for use in construction projects.

## 2. Materials and Methodology

### 2.1 Materials

The Ground Granulated Blast Furnace Slag (GGBS) operated in the role of geo-polymer precursors because of its significant calcium Concentration, crystalline structure and ability to produce strong compressive strength when cured at room temperature [15]. Zone II M-sand complying with standard grading requirements, served as the fine aggregate [16]. Similarly, specimens to test compressive strength were prepared and tested for those made of Ordinary Portland Cement (OPC) mortar. This investigated show that the impact of silicate content on the compressive strength of GGBS-based geo-polymer mortar by maintaining a constant sodium silicate composition while testing various Sodium Silicate to Sodium Hydroxide ratio combinations [17]. Table 1 presents the physical properties of GGBS and OPC used in this study.

**Table 1:** Physical Properties of GGBS and OPC

Physical Properties	GGBS	OPC
Specific Gravity	2.87	3.12
Color	Off-white	Grey
Fineness	High	Moderate
Soundness	< 10 mm	1.25 mm

### 2.2 Alkaline Activator Preparation

Solutions of sodium hydroxide 6M, 8M, 10M, 12M, and 14M. Solutions of 97% pure sodium hydroxide were prepared by dissolving in distilled water. Sodium hydroxide solutions of different molarities between 6M and 14M were created to depict low, medium, and high alkalinity levels. In order to achieve thermal stabilization and full dissolution, the NaOH solutions were made at least 24 hours before mixing the mortar. The alkaline activator by combining NaOH solution with commercially sodium silicate solution according to their established Sodium Silicate (SS) to Sodium Hydroxide (SH) ratio of 1:1, 2:1 and 3:1.[18].

### 2.3 Mix Proportioning

In this study six different Geo-polymer mortar mixes by using a constant binder-to-fine aggregate ratio of 1:3 and an unchanging alkaline liquid to binder ratio of 0.70 for their testing. The study maintained sodium hydroxide (NaOH) molarity between 6M and 14M while using sodium silicate (SS) to sodium hydroxide (SH) ratios of 1:1, 2:1 and 3:1 respectively [19]. Alkaline activator composition effects were identified and evaluated methodically on the formation of Compressive strength by holding all the other mix parameters unchanged.

**Table 2:** Mix Proportioning of Mortar Mix

Mix Id	Binder (B) (gm)	Sand (gm)	AL/B	Sodium Hydroxide (M)	SS/SH	Water (gm)
G6M-1	500	1500	0.7	6	1	-
G6M-2	500	1500	0.7	6	2	-
G6M-3	500	1500	0.7	6	3	-
G8M-1	500	1500	0.7	8	1	-
G8M-2	500	1500	0.7	8	2	-
G8M-3	500	1500	0.7	8	3	-
G10M-1	500	1500	0.7	10	1	-
G10M-2	500	1500	0.7	10	2	-
G10M-3	500	1500	0.7	10	3	-
G12M-1	500	1500	0.7	12	1	-
G12M-2	500	1500	0.7	12	2	-

G12M-3	500	1500	0.7	12	3	-
G14M-1	500	1500	0.7	13	1	-
G14M-2	500	1500	0.7	13	2	-
G14M-3	500	1500	0.7	13	3	-
OPC	500	1500	-	-	-	210

## 2.4 Mix Preparation, Specimen Casting, and Curing

GGBS and fine aggregate were dried and mix for 3 minutes, after dry mix addition of alkaline activator solution, and further mix of the same took place in 4 minutes[20]. The new mortar was poured into 70.6 mm cube-shaped molds, pressed up with a vibration table, demolded after 24 hours, and allowed to dry in the standard conditions of the laboratory (25-28°C) until the test[21].

## 2.5 Mechanical Strength (Compressive strength)

According to IS 516, the compressive strength was measured by Compression Testing Machine using a 3000KN standardized compression machine on 7 and 28 days [22]. Each cube was tested with the loading rate being controlled to about 2.9 KN/s, which is a standard loading rate for 70.6 mm cube specimens, and the machine learning based analysis was done with the average values of the strength[23]. The compressive strength testing setup of geo-polymer mortar cubes is illustrated in Figure 1.



Fig. 1. Experimental setup for compressive strength testing of geo-polymer mortar cubes

## 2.6 Methodology of machine learning

The data related to compressive strength was experimented with, and then it was applied using machine learning techniques. The input parameters were NaOH molarity and Alkaline-solution ratio, and compressive strength was an output variable. It divided the dataset into two different parts such as Training (80) and Testing (20). The models used for forecasting compressive strength and discovering non-linear relationships operated through Multiple linear regression (MLR) model, Random forest (RF) model, support vector regression (SVR) model and XG-Boost model implementations. Figure 2 shows that the machine learning (ML) general workflow used in this study was as follows. Tables 3 and 4 indicate that the model of machine learning is based on equations.

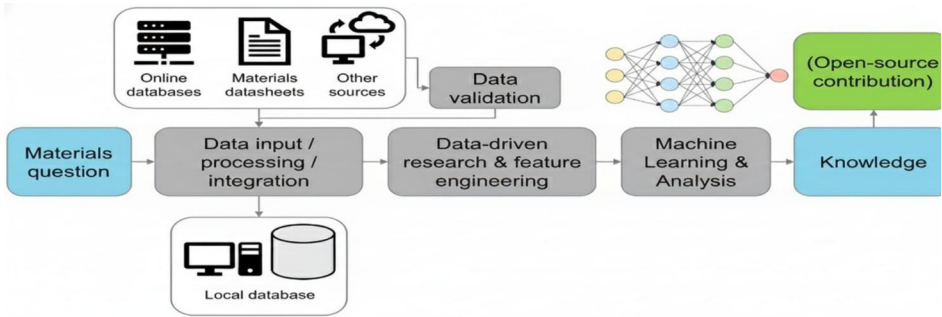


Fig. 2. Machine learning based on compressive strength flow chart [13]

Machine Learning Model Performance Evaluation Equations

1.  $R^2$  (Coefficient of Determination): Measures goodness of fit
2. RMSE (MPa): Penalizes large prediction errors
3. MAE (MPa): Average absolute prediction error

Table 3. Equations used of ML models at 7 days

Model	Equations			
	Predicted Strength	$R^2$	RMSE	MAE
Multiple Linear Regression	$\hat{f}_{c_7} = \beta_0^{(7)} + \beta_1^{(7)}(M) + \beta_2^{(7)}\left(\frac{SS}{SH}\right)$	$1 - \frac{\sum(f_{c_7} - \hat{f}_{c_7})^2}{\sum(f_{c_7} - \bar{f}_{c_7})^2}$	$\sqrt{\frac{1}{n} \sum (f_{c_7} - \hat{f}_{c_7})^2}$	$\frac{1}{n} \cdot \sum  f_{c_7} - \hat{f}_{c_7} $
Support Vector Machine	$\hat{f}_{c_7} = \sum_{i=1}^n (\alpha_i - \alpha_i^*) \exp(-\gamma \ x_i - x\ ^2) + b$	$1 - \frac{\sum(f_{c_7} - \hat{f}_{c_7})^2}{\sum(f_{c_7} - \bar{f}_{c_7})^2}$	$\sqrt{\frac{1}{n} \sum (f_{c_7} - \hat{f}_{c_7})^2}$	$\frac{1}{n} \cdot \sum  f_{c_7} - \hat{f}_{c_7} $
Random Forest	$\hat{f}_{c_7} = \frac{1}{T} \sum_{t=1}^T h_t \left\{ (M), \frac{SS}{SH} \right\}$	$1 - \frac{\sum(f_{c_7} - \hat{f}_{c_7})^2}{\sum(f_{c_7} - \bar{f}_{c_7})^2}$	$\sqrt{\frac{1}{n} \sum (f_{c_7} - \hat{f}_{c_7})^2}$	$\frac{1}{n} \cdot \sum  f_{c_7} - \hat{f}_{c_7} $
XG-Boost	$\hat{f}_{c_7} = \sum_{k=1}^K f_k \left\{ (M), \frac{SS}{SH} \right\}$	$1 - \frac{\sum(f_{c_7} - \hat{f}_{c_7})^2}{\sum(f_{c_7} - \bar{f}_{c_7})^2}$	$\sqrt{\frac{1}{n} \sum (f_{c_7} - \hat{f}_{c_7})^2}$	$\frac{1}{n} \cdot \sum  f_{c_7} - \hat{f}_{c_7} $

**Table 4.** Equations used of ML models at 28 days

Model	Equations			
	Predicted Strength	R <sup>2</sup>	RMSE	MAE
Multiple Linear Regression	$\hat{f}_{c_{28}} = \beta_0^{(28)} + \beta_1^{(28)}M + \beta_2^{(28)}\left(\frac{SS}{SH}\right)$	$1 - \frac{\sum(f_{c_{28}} - \hat{f}_{c_{28}})^2}{\sum(f_{c_{28}} - f_{c_{28}})^2}$	$\sqrt{\frac{1}{n} \sum (f_{c_{28}} - \hat{f}_{c_{28}})^2}$	$\frac{1}{n} \sum  f_{c_{28}} - \hat{f}_{c_{28}} $
Support Vector Machine	$\hat{f}_{c_{28}} = \sum_{i=1}^n (\alpha_i - \alpha'_i) \exp(-\gamma \ x_i - x\ ^2) + b$	$1 - \frac{\sum(f_{c_{28}} - \hat{f}_{c_{28}})^2}{\sum(f_{c_{28}} - f_{c_{28}})^2}$	$\sqrt{\frac{1}{n} \sum (f_{c_{28}} - \hat{f}_{c_{28}})^2}$	$\frac{1}{n} \sum  f_{c_{28}} - \hat{f}_{c_{28}} $
Random Forest	$\hat{f}_{c_{28}} = \frac{1}{T} \sum_{t=1}^T h_t \left\{ (M), \left(\frac{SS}{SH}\right) \right\}$	$1 - \frac{\sum(f_{c_{28}} - \hat{f}_{c_{28}})^2}{\sum(f_{c_{28}} - f_{c_{28}})^2}$	$\sqrt{\frac{1}{n} \sum (f_{c_{28}} - \hat{f}_{c_{28}})^2}$	$\frac{1}{n} \sum  f_{c_{28}} - \hat{f}_{c_{28}} $
XG-Boost	$\hat{f}_{c_{28}} = \sum_{k=1}^K f_k \left\{ (M), \left(\frac{SS}{SH}\right) \right\}$	$1 - \frac{\sum(f_{c_{28}} - \hat{f}_{c_{28}})^2}{\sum(f_{c_{28}} - f_{c_{28}})^2}$	$\sqrt{\frac{1}{n} \sum (f_{c_{28}} - \hat{f}_{c_{28}})^2}$	$\frac{1}{n} \sum  f_{c_{28}} - \hat{f}_{c_{28}} $

The predicted compressive strength on 7 ( $\hat{f}_{c_7}$ ) and 28 ( $\hat{f}_{c_{28}}$ ) days which were obtained through four Machine Learning (ML) Models Multiple Linear Regression (MLR) model, Support Vector Machine (SVM) model, Random Forest (RF) model and Extreme Gradient Boost (XG-Boost) model machine learning methods are presented in Tables 2 and 3. The models used sodium hydroxide molarity which ranged from 6M to 14M and sodium silicate (SS) to sodium hydroxide (SH) ratio as their basic input parameters. MLR model predicts strength based on its direct linear connection between input variables and compressed strength. SVM model includes a radial basis function (RBF) kernel to establish nonlinear connections between activator parameters and strength development. The RF algorithm creates several decision trees which generate predictions that the algorithm combines through averaging to enhance system performance while stopping overfitting. XG-Boost employs a gradient boosting method which integrates various weak predictive models to develop a final model that produces superior accurate results and better generalizes to different scenarios. The researchers employed statistical performance indicators which included R<sup>2</sup> and RMSE and MAE to assess and compare model performance. The system demonstrates better predictive performance because it achieved higher R<sup>2</sup> values together with lower RMSE and MAE results.

### 3. Results and Discussion

#### 3.1 NaOH concentration impact on Compressive Strength

Compressive strength development of geo-polymer mortar of GGBS at 7 and 28 days is show in Figures 3(a) and 3(b). Maximum compressive strength of 40 MPa was occurred after 7 days with the used of 10M Sodium Hydroxide Concentration and an alkaline activator ratio of 2, while Compressive strength after 28 days was approximately 60 MPa with the same activator composition. The changes in the alkaline activator ratio within all molarity levels showed only significant differences in compressive strength which was quite nonlinear. The strength of 6M mixes decreased when the alkaline activator ratio increased, while the 8M mixes showed strength improvement with higher alkaline activator ratios. The alkaline activator ratio of 2.0 maintained steady performance across all tested molarity levels.

The study found that increase sodium hydroxide concentration then compressive strength also increase from 6 M to 12 M because the higher sodium hydroxide concentration allowed more alumino-silicate compounds from GGBS to dissolve which resulted in faster calcium-alumino-silicate-hydrate gel produced that built a more compacted and resilient geo-polymer matrix. The complete collection of geo-polymerization reactions together with their ongoing process of gel densification under normal curing conditions has been verified through the strength measurements that occurred between the seventh and twenty-eighth day. The strength gain reached its peak when sodium hydroxide concentration increased to 14 M because excessive sodium hydroxide concentration prevented the polymerization process from proceeding at its normal rate. The research results demonstrate that sodium hydroxide concentration

nonlinearly affects the strength of geo-polymer mortar with the use of GGBS as a base material because the GGBS showed stable performance across all testing concentration levels.

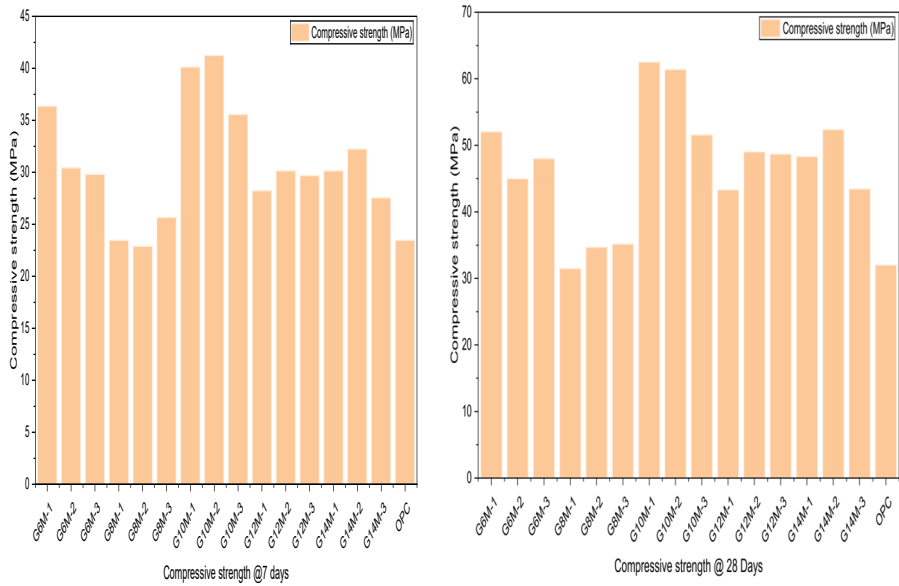


Fig. 3. Compressive strength on various NaOH molarity at 7 and 28 days.

### 3.2 Machine Learning Prediction on Compressive Strength

Machine learning models used Molarity and SS/SH ratio as effective inputs which produced better results for predicting compressive strength through their ensemble-based algorithms. The predicted results demonstrated excellent correlation with experimental data which confirmed that machine learning models outperformed traditional regression techniques because they extracted complex relationships present in geo-polymer systems.

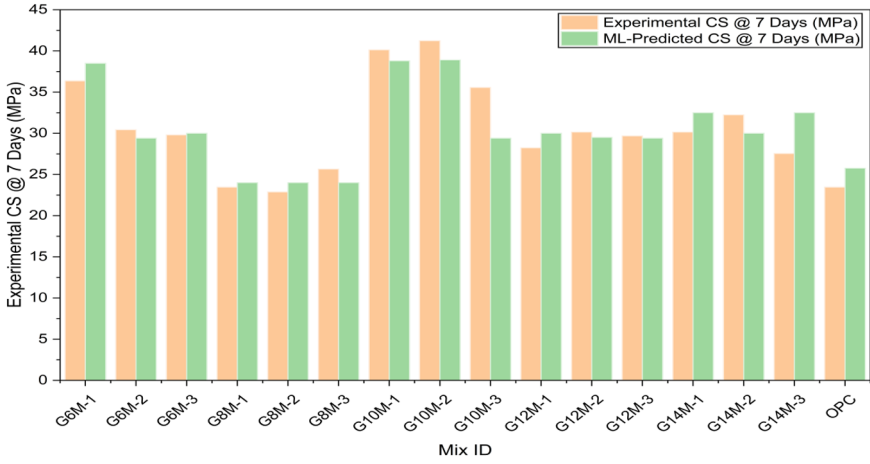


Fig. 4. Compressive strength based on Experimental and Machine Learning predicted at 7 days

The experimental results and machine learning predictions show compressive strength at 7-day testing in Figure 4. The data point's show tight grouping which proved that the Random Forest model accurately predicted early strength development based the alkaline activators molarity.

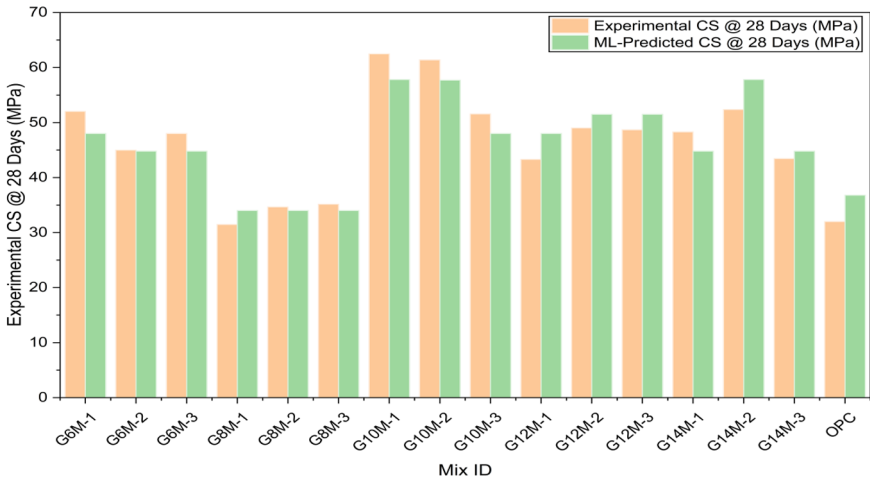


Fig. 5. Compressive strength based on Experimental and Machine Learning predicted at 28 days

In Figure 5, the experimental and predicted 28 day compressive strengths are related. The excellent fit of both predicted and experimental values indicates the soundness of the machine learning model in modeling long-term strength behavior and the nonlinear relationship between molarity of NaOH and strength.

**Table 5:** Compressive strength prediction using Machine Learning models after 7 days

Model	R <sup>2</sup>	RMSE (MPa)	MAE (MPa)
Multiple Linear Regression	0.83	3.45	2.98
Support Vector Machine	0.94	2.61	2.14
Random Forest	1.1	1.78	1.32
XG-Boost	1.0	1.54	1.18

Table 5. Synthesizes the forecasting ability of various machine-level models of 7 day compressive strength. Linear regression lacks accuracy as a result of nonlinearity. The ensemble models, especially model of XG-Boost and random forest, are more effective as they have higher R<sup>2</sup> and lower error value, which proves that they are effective in predicting the strength of a structure at an early age.

**Table 6:** Compressive strength prediction using Machine Learning models after 7 days

Model	R <sup>2</sup>	RMSE (MPa)	MAE (MPa)
Multiple Linear Regression	0.85	4.12	3.36
Support Vector Machine	0.92	2.94	2.21
Random Forest	0.97	1.96	1.45
XG-Boost	0.98	1.63	1.21

The table 6 shows that the compressive strength prediction based on Machine Learning algorithms after 28 days. The models show results after stabilization of geo-polymerization because all testing models need to prove their effectiveness at high-precision testing. The XG-Boost model reaches its best accuracy which demonstrates its capacity to model complex non-linear relationships in strength development over an extended period.

### 3.3 Performance Comparison of Machine Learning (ML) Models

XG-Boost model, random forest algorithms outperformed Support Vector Regression and MLR through their higher prediction accuracy and lower error rates. The system demonstrates superior performance because its ensemble

learning methods effectively track complex relationships between molarity and compressive strength. The results show that data-driven methods effectively optimize geo-polymer mix compositions.

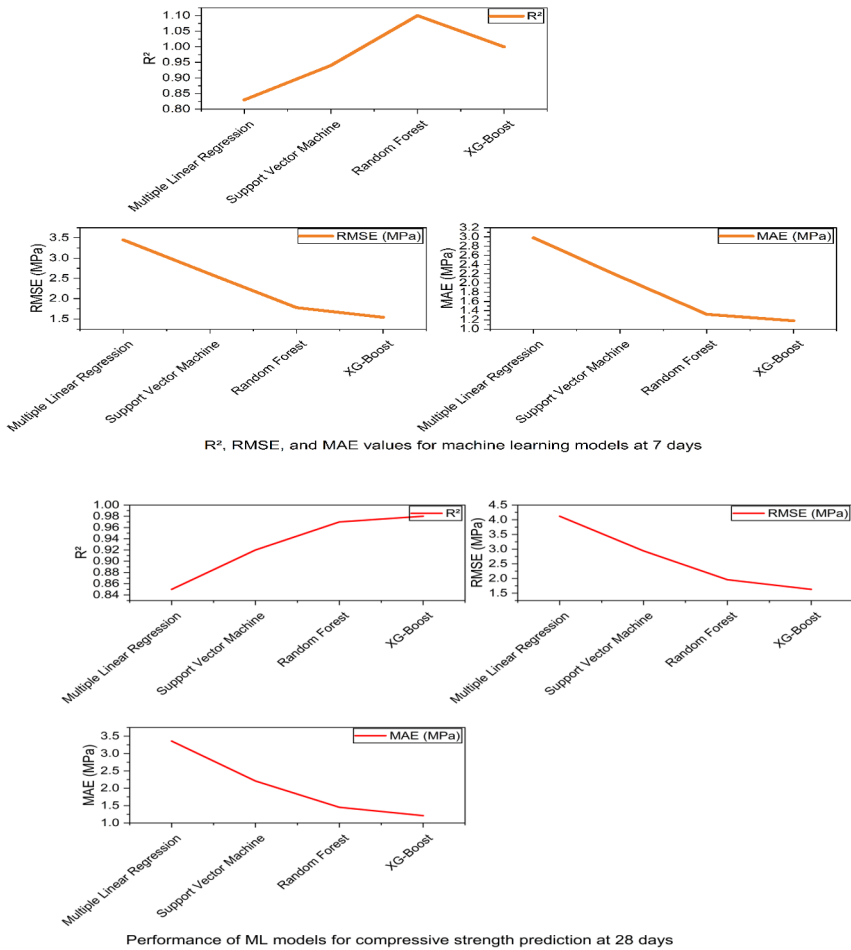


Fig. 6: Comparison of  $R^2$ , RMSE, and MAE values for machine learning models at 7 and 28 day

In fig. 6. Show that the study results reveal which machine learning model performs better because they analyzed both 7-day and 28-day testing results which showed different prediction accuracy results and error measurement outcomes. The Multiple Linear Regression (MLR) model demonstrates its worst predictive ability through its curing results because it shows the lowest  $R^2$  values and the highest RMSE and MAE values which show its power to predict strength growth results. The Support Vector Machine (SVM) model has a better performance than the MLR with average  $R^2$  values and smaller error measures; it still has a larger error in prediction as compared to the ensemble-based models.

Random Forest shows extremely strong performance through its  $R^2$  values which range from 0.96 to 0.97 and its exceptionally low RMSE and MAE results for both 7-day and 28-day tests because it can handle complex relationships between input variables. The research results demonstrate that advanced ensemble models which include XG-Boost and Random Forest provide better predictions of compressive strength development than traditional regression-based methods at advanced curing stages.

#### 3.4 Observations from Experimental and ML Analysis

1. A nonlinear higher compressive strength was observed during 6M to 14M NaOH Concentration.
2. Maximum compressive strength was determined for a molarity in the range of 10-12 M.
3. 28-day compressive strength improved by approximately 25–30% at higher molarity compared to low-molarity mixes
4. Machine learning models predicted compressive strength with  $R^2 > 0.95$
5. XG-Boost and Random Forest models showed the lowest prediction errors
6. Ensemble learning models outperformed linear and kernel-based regression techniques

#### 4. Conclusion

The research conducted an experimental study which used data-driven machine learning methods to examine how GGBS-based geo-polymer mortar compressive strength developed with different alkaline activator molarity levels. The researchers tested sodium hydroxide molarity between 6 M and 14 M while keeping all other mix parameters fixed to study how sodium hydroxide affected strength development. The experimental findings demonstrated that the alkaline activator molarity determines the geo-polymerization kinetics and the development of compressive strength during ambient curing conditions.

1. The experimental study found that geo-polymer mortars prepared with lower molarity levels (6–8 M) showed reduced compressive strength because their alkalinity levels were not sufficient to dissolve GGBS particles effectively.
2. The compressive strength values for low-molarity mixes reached 22 to 30 MPa at 7 days, while the 10 to 14 M higher molarity mixes achieved early-age strengths that exceeded 35 MPa.
3. The compressive strength of the material reached its highest value at 28 days through a continuous strength increase which depended on molarity until it achieved approximately 60–62 MPa at the 10–14 M range whereas the 6–8 M mixes produced results below 45 MPa. The study showed that higher molarity levels provided about 25–30 percent better long-term compressive strength results to the researchers. The strength gain showed a nonlinear pattern which showed only slight strength improvement after the 12–14 M point because this point established a maximum effective molarity level for the testing.
4. The machine learning part of the research proved that data-based models could correctly forecast compressive strength through their use of minimal test data. The study results showed that XG-Boost and Random Forest models achieved better performance than Multiple Linear Regression (MLR) model and Support Vector Machine (SVM) model.
5. At 7 days, the prediction analysis of XG-Boost showed ( $R^2 = 0.97$ ) extraordinarily accurate results with low error values (RMSE = 1.54 MPa, MAE = 1.18 MPa).
6. The best results at 28 days testing XG-Boost constructed from  $R^2 = 0.98$  and RMSE = 1.63 MPa and MAE=1.2MPa showed perfect correlation between its predicted results and actual testing data. Ensemble-based models achieve better results because they successfully model the intricate nonlinear relationships that exist between alkaline activator molarity and compressive strength.

7. This research establishes that combining experimental testing with machine learning techniques provides a robust and efficient framework for geo-polymer mortar optimization.
8. The proposed AI-assisted methodology significantly reduces experimental effort while maintaining high prediction reliability, thereby supporting sustainable and intelligent mix design strategies.
9. The findings contribute to advancing the practical implementation of GGBS-based geo-polymer mortars as low-carbon alternatives to conventional cementitious materials.

## References

- [1] C. Meyer, "The greening of the concrete industry," *Cem. Concr. Compos.*, vol. 31, no. 8, pp. 601–605, 2009, doi: 10.1016/j.cemconcomp.2008.12.010.
- [2] D. N. Huntzinger and T. D. Eatmon, "A life-cycle assessment of Portland cement manufacturing: comparing the traditional process with alternative technologies," *J. Clean. Prod.*, vol. 17, no. 7, pp. 668–675, 2009, doi: 10.1016/j.jclepro.2008.04.007.
- [3] Z. He, X. Zhu, J. Wang, M. Mu, and Y. Wang, "Comparison of CO<sub>2</sub> emissions from OPC and recycled cement production," *Constr. Build. Mater.*, vol. 211, pp. 965–973, 2019, doi: 10.1016/j.conbuildmat.2019.03.289.
- [4] J. Davidovits, "Properties of Geopolymer Cements," *First Int. Conf. Alkaline Cem. Concr.*, pp. 131–149, 1994.
- [5] A. E. Alexander and A. P. Shashikala, "Studies on the microstructure and durability characteristics of ambient cured FA-GGBS based geopolymer mortar," *Constr. Build. Mater.*, vol. 347, no. June, p. 128538, 2022, doi: 10.1016/j.conbuildmat.2022.128538.
- [6] M. H. Al-Majidi, A. Lampropoulos, A. Cundy, and S. Meikle, "Development of geopolymer mortar under ambient temperature for in situ applications," *Constr. Build. Mater.*, vol. 120, pp. 198–211, 2016, doi: 10.1016/j.conbuildmat.2016.05.085.
- [7] A. E. Kurtoğlu *et al.*, "Mechanical and durability properties of fly ash and slag based geopolymer concrete," *Adv. Concr. Constr.*, vol. 6, no. 4, pp. 345–362, 2018, doi: 10.12989/acc.2018.6.4.345.
- [8] "Study on the initial curing condition fly ash and GGBS recycled aggregate concrete.pdf."
- [9] G. S. Ryu, Y. B. Lee, K. T. Koh, and Y. S. Chung, "The mechanical properties of fly ash-based geopolymer concrete with alkaline activators," *Constr. Build. Mater.*, vol. 47, no. 2013, pp. 409–418, 2013, doi: 10.1016/j.conbuildmat.2013.05.069.
- [10] G. Mallikarjuna Rao and T. D. Gunneswara Rao, "Final Setting Time and Compressive Strength of Fly Ash and GGBS-Based Geopolymer Paste and Mortar," *Arab. J. Sci. Eng.*, vol. 40, no. 11, pp. 3067–3074, 2015, doi: 10.1007/s13369-015-1757-z.
- [11] L. N. Assi, E. Deaver, M. K. Elbatanouny, and P. Ziehl, "Investigation of early compressive strength of fly ash-based geopolymer concrete," *Constr. Build. Mater.*, vol. 112, pp. 807–815, 2016, doi: 10.1016/j.conbuildmat.2016.03.008.
- [12] A. E. Alexander and A. P. Shashikala, "Studies on the microstructure and durability characteristics of ambient cured FA-GGBS based geopolymer mortar," *Constr. Build. Mater.*, vol. 347, no. July, p. 128538, 2022, doi: 10.1016/j.conbuildmat.2022.128538.
- [13] S. Philip, M. Nidhi, and H. U. Ahmed, "A comparative analysis of tree-based machine learning algorithms for predicting the mechanical properties of fibre-reinforced GGBS geopolymer concrete," *Multiscale Multidiscip. Model. Exp. Des.*, vol. 7, no. 3, pp. 2555–2583, 2024, doi: 10.1007/s41939-023-00355-6.
- [14] Z. Kurt, Y. Yilmaz, T. Cakmak, and I. Ustabaş, "A novel framework for strength prediction of geopolymer mortar: Renovative precursor effect," *J. Build. Eng.*, vol. 76, no. June, 2023, doi: 10.1016/j.job.2023.107041.

- [15] A. Mehta and K. Kumar, "Strength and durability characteristics of fly ash and slag based geopolymer concrete," *Int. J. Civ. Eng. Technol.*, vol. 7, no. 5, pp. 305–314, 2016.
- [16] A. Ojha and L. Gupta, "Comparative study on mechanical properties of conventional and geo-polymer concrete with recycled coarse aggregate," *Mater. Today Proc.*, vol. 28, no. xxxx, pp. 1403–1406, 2020, doi: 10.1016/j.matpr.2020.04.811.
- [17] Z. Tang, W. Li, V. W. Y. Tam, and Z. Luo, "Investigation on dynamic mechanical properties of fly ash/slag-based geopolymeric recycled aggregate concrete," *Compos. Part B Eng.*, vol. 185, p. 107776, 2020, doi: 10.1016/j.compositesb.2020.107776.
- [18] J. Xie, W. Chen, J. Wang, C. Fang, B. Zhang, and F. Liu, "Coupling effects of recycled aggregate and GGBS/metakaolin on physicochemical properties of geopolymer concrete," *Constr. Build. Mater.*, vol. 226, pp. 345–359, 2019, doi: 10.1016/j.conbuildmat.2019.07.311.
- [19] B. Gopalakrishna and P. Dinakar, "Mix design development of fly ash-GGBS based recycled aggregate geopolymer concrete," *J. Build. Eng.*, vol. 63, no. PA, p. 105551, 2023, doi: 10.1016/j.job.2022.105551.
- [20] A. Sales *et al.*, "Mechanical properties of concrete produced with a composite of water treatment sludge and sawdust Related papers Durability of Concrete with Recycled Coarse Aggregates: Influence of Superplasticizers MECHANICAL PROPERTIES OF CONCRETE PRODUCED WITH RE".
- [21] P. Saravanakumar, "Strength and durability studies on geopolymer recycled aggregate concrete," *Int. J. Eng. Technol.*, vol. 7, no. 2, pp. 370–375, 2018, doi: 10.14419/ijet.v7i2.24.12087.
- [22] O. A. Mohamed, R. Al Khattab, and W. Al Hawat, "Effect of relative GGBS/fly contents and alkaline solution concentration on compressive strength development of geopolymer mortars subjected to sulfuric acid," *Sci. Rep.*, vol. 12, no. 1, pp. 1–13, 2022, doi: 10.1038/s41598-022-09682-z.
- [23] P. Kathirvel and S. R. M. Kaliyaperumal, "Influence of recycled concrete aggregates on the flexural properties of reinforced alkali activated slag concrete," *Constr. Build. Mater.*, vol. 102, pp. 51–58, 2016, doi: 10.1016/j.conbuildmat.2015.10.148.

**Open Access** This chapter is licensed under the terms of the Creative Commons Attribution-NonCommercial 4.0 International License (<http://creativecommons.org/licenses/by-nc/4.0/>), which permits any noncommercial use, sharing, adaptation, distribution and reproduction in any medium or format, as long as you give appropriate credit to the original author(s) and the source, provide a link to the Creative Commons license and indicate if changes were made.

The images or other third party material in this chapter are included in the chapter's Creative Commons license, unless indicated otherwise in a credit line to the material. If material is not included in the chapter's Creative Commons license and your intended use is not permitted by statutory regulation or exceeds the permitted use, you will need to obtain permission directly from the copyright holder.

